

# Morphological study of stabilization and carbonization of polyacrylonitrile/TiO<sub>2</sub> nanofiber mats

Lilia Sabantina<sup>1,2</sup>, Robin Böttjer<sup>1</sup>, Daria Wehlage<sup>1</sup>,  
Timo Grothe<sup>1</sup>, Michaela Klöcker<sup>1</sup>, Francisco José García-Mateos<sup>2</sup>,  
José Rodríguez-Mirasol<sup>2</sup>, Tomás Cordero<sup>2</sup> and Andrea Ehrmann<sup>1</sup>

## Abstract

Polyacrylonitrile belongs to the most often used precursors for carbon fibers. Using electrospinning, polyacrylonitrile nanofiber mats can be prepared and afterwards stabilized and carbonized to prepare carbon nanofiber mats which, by adding other materials, will be useful for several applications. One of these materials is TiO<sub>2</sub>, which has photocatalytic properties and can thus be used as a photocatalyst for photodegradation of dyes. Here, we report on a detailed study of electrospinning, stabilization, and carbonization of electrospun polyacrylonitrile/TiO<sub>2</sub> mats with varying TiO<sub>2</sub> content. Depending on the amount of TiO<sub>2</sub> in the nanofibers, the fiber morphology changes strongly, indicating an upper limit for the preparation of carbon/TiO<sub>2</sub> nanofibers with smooth surface, but offering an even increased inner surface of the rougher carbon/TiO<sub>2</sub> nanofibers with increased TiO<sub>2</sub> content due to better maintenance of the fibrous structure during stabilization.

## Keywords

Polyacrylonitrile, PAN, TiO<sub>2</sub>, nanofiber mat, electrospinning, composite, stabilization, carbonization

Date received: 22 April 2019; accepted: 17 June 2019

## Introduction

Electrospinning is a method often used to prepare nanofibers or nanofiber mats.<sup>1–3</sup> Due to their large surface-to-volume ratio, such nanofiber mats are used for diverse applications, from filter materials<sup>4,5</sup> to catalysts<sup>6–8</sup> to medical wound dressing.<sup>9</sup> Besides pure polymers, also polymer blends or polymers with incorporated inorganic compounds can be electrospun.<sup>10–12</sup>

A polymer which has been studied often is polyacrylonitrile (PAN). On one hand, it can be used as a precursor for carbon nanofibers;<sup>13–16</sup> on the other hand, it can be spun from low-toxic dimethyl sulfoxide (DMSO)<sup>17</sup> which is especially advantageous for biotechnological applications.<sup>18</sup>

Carbonizing PAN nanofibers with included inorganic materials can be used to broaden the possible applications

of such composites. TiO<sub>2</sub> is of special interest as inorganic partner due to its photocatalytic properties.<sup>19–21</sup> Song et al.,<sup>22</sup> for example, used electrospun TiO<sub>2</sub>/carbon nanofiber mats to reach high photocatalytic degradation efficiency tested with rhodamine B and proved a high durability of this effect. Similarly, composites from leaf-shaped TiO<sub>2</sub> and reduced graphene oxide with

<sup>1</sup>Faculty of Engineering and Mathematics, Bielefeld University of Applied Sciences, Bielefeld, Germany

<sup>2</sup>Andalucía Tech, Departamento de Ingeniería Química, Universidad de Málaga, Málaga, Spain

### Corresponding author:

Andrea Ehrmann, Faculty of Engineering and Mathematics, Bielefeld University of Applied Sciences, Bielefeld 33619, Germany.  
Email: andrea.ehrmann@fh-bielefeld.de



approximately 1% of reduced graphene oxide showed large photocatalytic activity.<sup>23</sup> However, anodes for lithium-ion batteries were produced from  $\alpha$ -Fe<sub>2</sub>O<sub>3</sub> grains grafted on TiO<sub>2</sub>/carbon nanofibers,<sup>24</sup> N-doped TiO<sub>2</sub>/carbon nanofibers were used as anodes in sodium-ion batteries,<sup>25</sup> and carbon/TiO<sub>2</sub> nanofibers were used as negative electrodes for vanadium redox flow batteries.<sup>26</sup>

Typically, TiO<sub>2</sub>/carbon nanofibers are electrospun from a solution of titanium tetraisopropoxide, solvent, and polymer.<sup>24,27</sup> Since titanium tetraisopropoxide (Ti{OCH(CH<sub>3</sub>)<sub>2</sub>}<sub>4</sub>) is flammable and slightly toxic, however, it must be handled with care if used in a needleless electrospinning machine, spinning with high voltages up to 80 kV. Alternatively, tetra-*n*-butyl titanate (Ti(C<sub>4</sub>H<sub>9</sub>O)<sub>4</sub>) can be used,<sup>23,25,26</sup> a material which is also flammable and in addition, corrosive and toxic. Only few reports can be found in the literature about coating electrospun nanofibers with TiO<sub>2</sub> nanoparticles;<sup>28–31</sup> however, immobilization of the TiO<sub>2</sub> particles on the nanofiber surface is not easy.

Including TiO<sub>2</sub> nanoparticles directly in the polymer solution is scarce. Chang et al.<sup>32</sup> report on needle-electrospinning from dimethylformamide (DMF) as the solvent, using a TiO<sub>2</sub>:PAN weight ratio of 1:10. While the original electrospun nanofibers show a relatively even rough surface, self-erosion of the embedded TiO<sub>2</sub> particles results in several large holes along the fibers which become larger during carbonization. An et al.<sup>33</sup> investigated three different weight ratios of TiO<sub>2</sub>:PAN/PVP (from 3.4% to 13.8% of the precursor solution; the polymer content is not given) for the possible use as counter electrodes in dye-sensitized solar cells. By needle electrospinning this solution from DMF as the solvent, nanofibers with different surface roughness were gained. Electrospinning from a polyphenylene vinylene (PPV) solution containing TiO<sub>2</sub> was reported by Wang et al.,<sup>34</sup> resulting in rough nanofibers in a broad range of diameters.

A systematic study of the morphological changes due to inclusion of different amounts of TiO<sub>2</sub> in polymer nanofibers, however, is still missing. The aim of this study is to thus investigate PAN nanofiber mats, needleless electrospun from DMSO—which was to the best of our knowledge not yet reported in the literature—with different amounts of TiO<sub>2</sub> in the spinning solution. The stabilization process which is known to significantly influence the nanofiber mat morphology by modifying stabilization temperatures and heating rates<sup>35</sup> is examined in detail, before some exemplary nanofiber mats are carbonized at different temperatures. The changes of the nanofiber mats due to these processing steps are important to understand for all applications of carbon/TiO<sub>2</sub> nanofiber mats, such as dye-sensitized solar cells or batteries.

## Materials and methods

Nanofiber mats were produced with the needleless electrospinning machine Nanospider Lab (Elmarco, Czech

Republic). The spinning parameters were as follows: high voltage 70 kV, electrode-substrate distance 240 mm, nozzle diameter 0.8 mm, carriage speed 100 mm/s, using a static substrate, relative humidity 33%, and temperature 21°C. It should be mentioned that the necessary relative humidity depends on the electrospinning technology and the electrospun polymer; in case of the Nanospider, working with a wire-based technology, a maximum humidity of 33% is ideal for spinning PAN, while higher relative humidity results in cotton-candy-like undesired structures.<sup>17</sup>

For the spinning solution, 16 wt% PAN were dissolved in DMSO (minimum 99.9% purity; S3 Chemicals, Germany); 0–10.2 wt% TiO<sub>2</sub> P25 nanoparticles (Degussa, Germany) were added to this solution. Solutions with higher amounts of TiO<sub>2</sub> could not be electrospun with the wire-based technology of the Nanospider Lab.

Stabilization of the samples was performed in a muffle furnace B150 (Nabertherm, Germany), approaching temperatures from 120°C to 300°C by heating rates between 0.5°C/min and 8°C/min, followed by isothermal treatment for 1 h. Opposite to a former experiment,<sup>35</sup> the samples were not fixed during this process to enable investigation of the influence of the TiO<sub>2</sub> content on the morphology change during this process. A furnace CTF 12/TZF 12 (Carbolite Gero Ltd., UK) was used for carbonization at 500°C or 800°C, approached with a heating rate of 10°C/min.

The sample morphology was investigated by a scanning electron microscope (SEM) Zeiss 1450VPSE, using a nominal magnification of  $\times 5000$ . An Excalibur 3100 (Varian, Inc., USA) was applied for Fourier-transform infrared (FTIR) spectroscopy. Sample masses were taken with an analytical balance (VWR, Radnor, Pennsylvania, USA).

## Results and discussion

In this section, SEM images of nanofiber mats after electrospinning, stabilization, and carbonization are shown, followed by chemical investigations using FTIR.

The first examinations concentrate on the morphology of the nanofibers. Figure 1 depicts the nanofiber mats electrospun with increasing amounts of TiO<sub>2</sub> (Figure 1(a)–(e)). While for the lowest amount of TiO<sub>2</sub> (Figure 1(a)), the fibers are mostly relatively smooth, straight, and regular, like pure PAN nanofiber mats,<sup>16,35</sup> more and thicker beads become visible for higher TiO<sub>2</sub> concentrations. These beads are typically visible if electrospinning is performed from solutions based on DMSO or other slowly evaporating solvents with relatively low solid content. Recent investigations of electrospinning PAN from DMSO with the Nanospider showed such beads for concentrations up to 15% solid content,<sup>14</sup> while they vanished for concentrations of 16% or higher. Here, these beads seem to be related to TiO<sub>2</sub> agglomerations which are surrounded by the polymer, according to the relatively uneven surface of

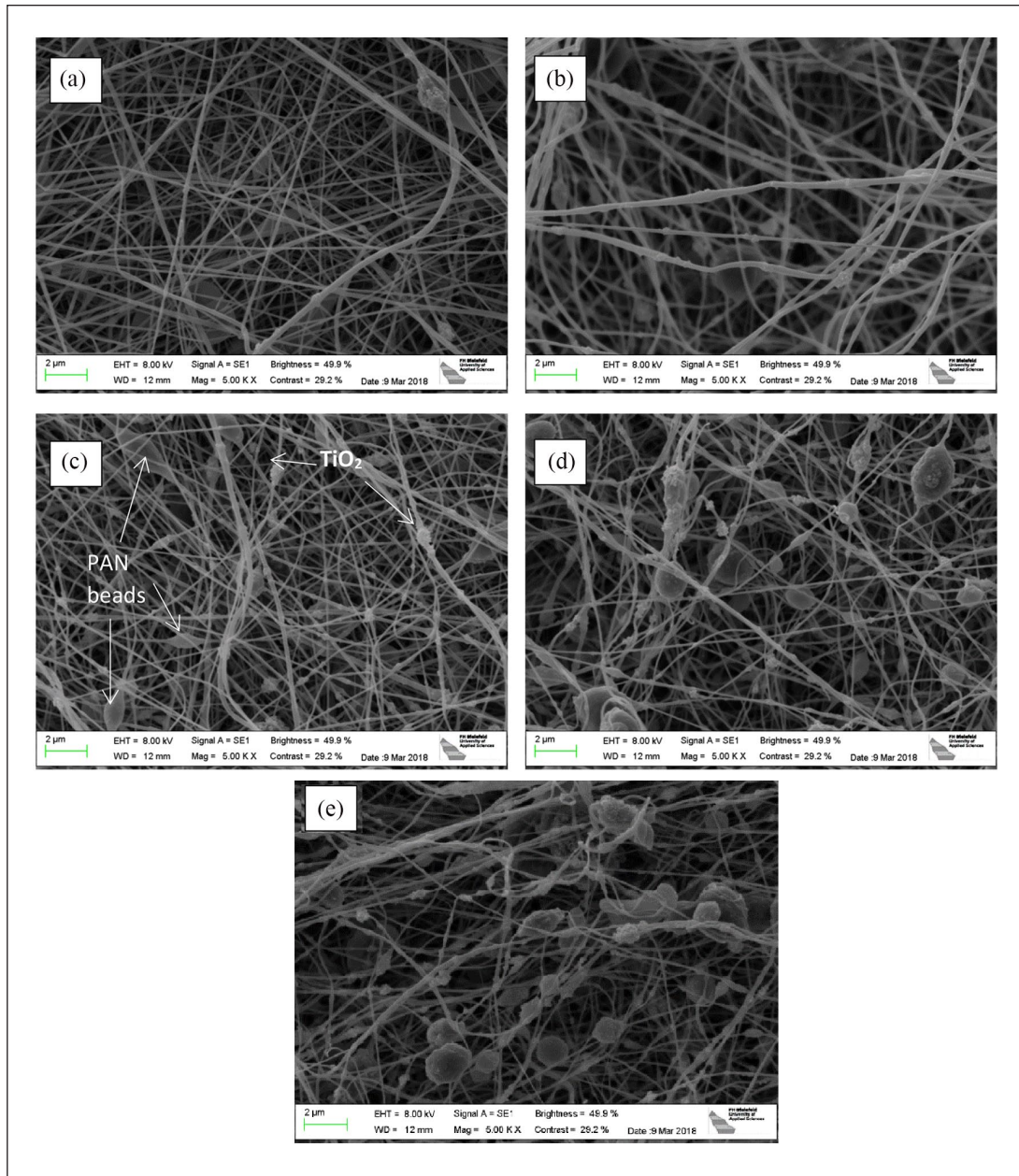


**Figure 1.** SEM images of PAN nanofiber mats with different amounts of  $\text{TiO}_2$  after electrospinning: (a) 2.2%  $\text{TiO}_2$ , (b) 4.2%  $\text{TiO}_2$ , (c) 6.2%  $\text{TiO}_2$ , (d) 8.2%  $\text{TiO}_2$ , and (e) 10.2%  $\text{TiO}_2$ .

the beads visible in Figure 1(e), indicating that they contain more  $\text{TiO}_2$  than the smooth fibers.

The overall fiber diameter is not visibly changed from the lowest  $\text{TiO}_2$  content ( $91 \pm 25$  nm) to the highest one ( $85 \pm 16$  nm), but the images show that the fibers are decorated with  $\text{TiO}_2$  nanoparticles or small agglomerations. It should be mentioned that in comparison with the literature, the amounts of  $\text{TiO}_2$  depicted here are relatively high (12.1%–38.9%) as compared to Wang et al.<sup>30</sup> (11.7%) in which the  $\text{TiO}_2$  nanoparticles were mostly embedded in the polymer fibers.

The nanofiber mats presented in Figure 1 were now stabilized at different temperatures, using a heating rate of  $1^\circ\text{C}/\text{min}$ . Figure 2 depicts the morphologies for a stabilization temperature of  $280^\circ\text{C}$ , the temperature found to be ideal to stabilize needleless electrospun PAN nanofiber mats without  $\text{TiO}_2$ .<sup>35</sup> The samples were not fixed during stabilization which lead to a typical change of the morphology toward meandering fibers with conglutinations along the crossing points,<sup>16,35</sup> also resulting in more visible beads per depicted area. This result is also visible here. However, here it may be recognized as a positive effect

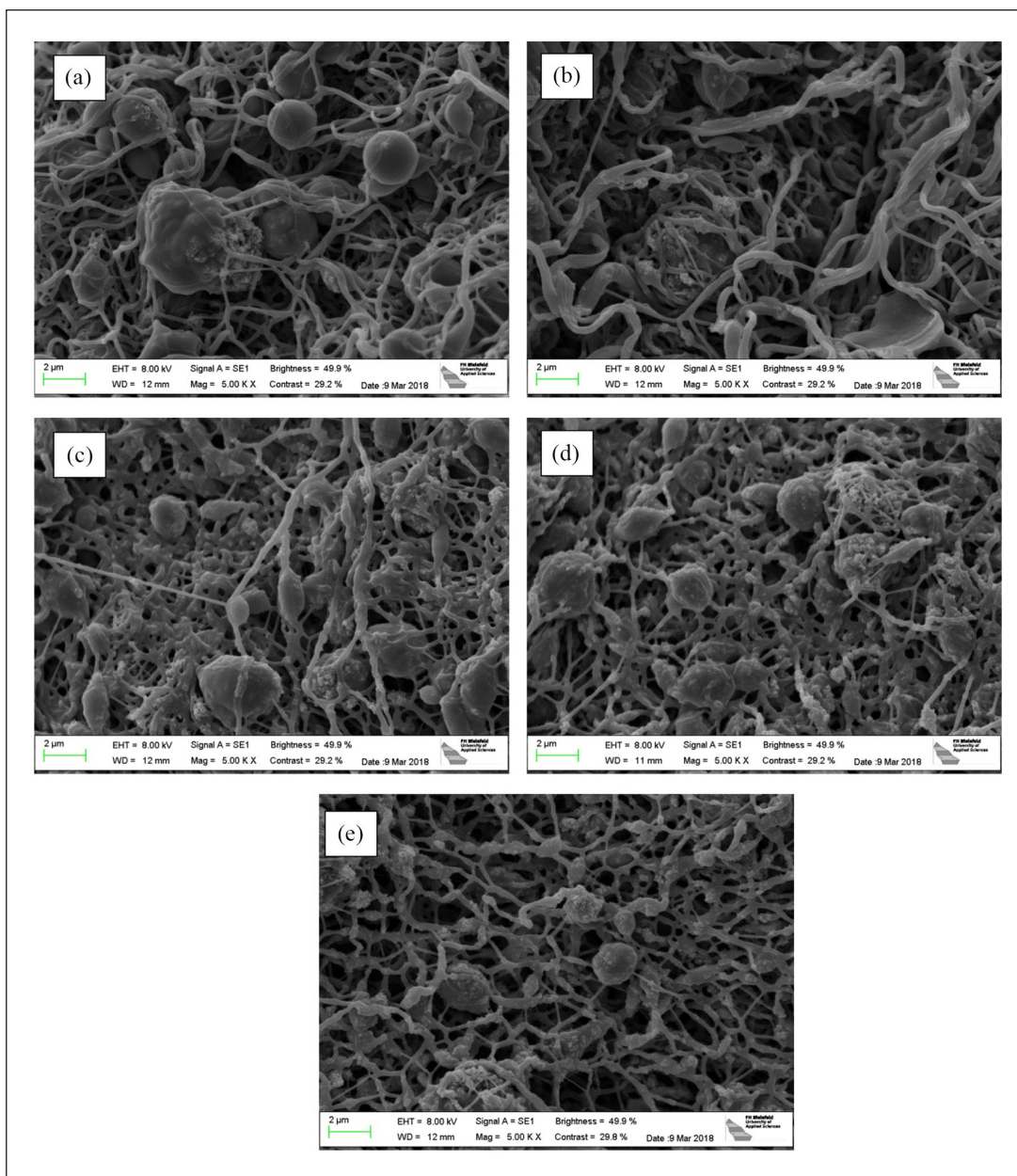


**Figure 2.** SEM images of PAN nanofiber mats with different amounts of  $\text{TiO}_2$  after stabilization at  $280^\circ\text{C}$ , approached with  $1^\circ\text{C}/\text{min}$ : (a) 2.2%  $\text{TiO}_2$ , (b) 4.2%  $\text{TiO}_2$ , (c) 6.2%  $\text{TiO}_2$ , (d) 8.2%  $\text{TiO}_2$ , and (e) 10.2%  $\text{TiO}_2$ .

since the fiber decoration by  $\text{TiO}_2$  nanoparticles becomes more regular during stabilization. In addition, fewer conglutinations are visible in the nanofiber mats with the highest  $\text{TiO}_2$  content.

An interesting finding is depicted in Figure 3, comparing the nanofiber mat with the highest  $\text{TiO}_2$  content after stabilization at  $280^\circ\text{C}$ , approached with heating rates of  $0.5^\circ\text{C}/\text{min}$  and  $8^\circ\text{C}/\text{min}$ . While such different heating rates resulted in significantly different morphologies for pure PAN, with large conglutination areas for high heating rates,<sup>35</sup> here both mats look similar. Apparently, the large amount of  $\text{TiO}_2$  stabilizes the nano-structure to a certain

extent, similar to the nearly complete conversion of the fiber structure by metal nanoparticles.<sup>36</sup>

The nanofiber mats stabilized at  $280^\circ\text{C}$  with a heating rate of  $1^\circ\text{C}/\text{min}$  were afterwards carbonized. Some results are depicted in Figure 4. As already expected from Figure 2, the strongest conglutinations are visible in the nanofiber mats with smallest  $\text{TiO}_2$  content, while for the highest  $\text{TiO}_2$  content, the nanofibers meander stronger and are obviously decorated with  $\text{TiO}_2$  nanoparticles in a relatively regular way, but have kept their original fiber structure instead of melting to form a more membrane-like structure, as it is visible for the samples with the lowest  $\text{TiO}_2$

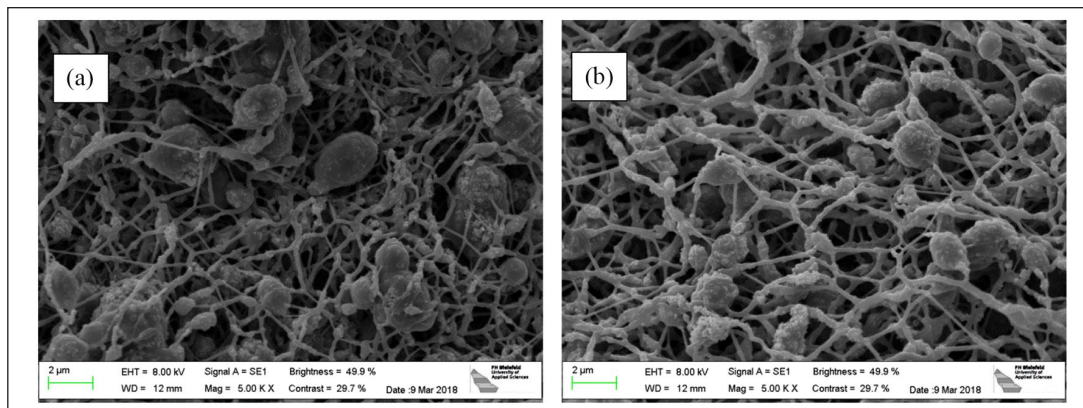


**Figure 3.** SEM images of PAN nanofiber mats with 10.2% TiO<sub>2</sub> after stabilization at 280°C, approached with different heating rates: (a) 0.5°C/min and (b) 8°C/min.

content. Carbonized pure PAN nanofiber mats are visible in Sabantina and colleagues.<sup>16,35</sup>

For a chemical examination, Figure 5(a) depicts the results of FTIR measurements directly after electrospinning. In all samples, the typical PAN absorbance peaks are visible: a stretching vibration of the C≡N nitrile functional group at 2240 cm<sup>-1</sup>, a carbonyl (C=O) stretching peak at 1732 cm<sup>-1</sup>, ester (C–O and C–O–C) vibrations of the co-monomers like itaconic acid or methyl acrylate which are often applied in industrial production of PAN occurring in the ranges of 1230–1250 cm<sup>-1</sup> and 1050–1090 cm<sup>-1</sup>, and bending and stretching vibrations of CH<sub>2</sub> at 2938, 1452, and 1380 cm<sup>-1</sup>.<sup>37</sup> In addition, the strong peak approximately below 880 cm<sup>-1</sup> can be attributed to TiO<sub>2</sub>.

During stabilization, most of these peaks are exchanged by new ones (Figure 5(b)): large peaks of C=N stretching vibrations at 1582 cm<sup>-1</sup> and C=C stretching vibration at 1660 cm<sup>-1</sup><sup>37</sup> as well as C–H bending and C–H<sub>2</sub> wagging at 1360 cm<sup>-1</sup>.<sup>38</sup> The peak around 800 cm<sup>-1</sup> can be attributed to aromatic C–H vibrations originating from oxidative dehydrogenation aromatization in the presence of oxygen.<sup>39</sup> Comparing this stabilization behavior with the temperature dependence of pure PAN nanofiber mats,<sup>35</sup> no differences of the stabilized states are visible. Further FTIR measurements are thus not shown here.

The influence of stabilization temperatures between 120°C and 300°C and heating rates between 0.5°C/min and 8°C/min on the mass yield after stabilization is depicted in Figure 6. For all amounts of TiO<sub>2</sub>, masses are relatively stable in the temperature range between 120°C and 240°C. The small mass loss can mostly be attributed to a drying process. For higher temperatures of 260°C to 300°C, a higher mass loss is visible, based on the chemical stabilization process itself. This finding is qualitatively and quantitatively similar to the few available reports on stabilization temperature-dependent carbon yield of pure PAN samples or PAN/gelatin samples.<sup>35,40</sup>

Investigating the influence of the heating rate on the mass loss (Figure 6(b)), nearly no impact of this value is visible. Only for the lowest heating rate, slightly smaller mass ratios are visible, but the differences are not significant, similar to the previous experiments with pure PAN nanofiber mats.<sup>35</sup> An influence of the TiO<sub>2</sub> concentration cannot be recognized either.

After carbonization at 500°C, a material yield of 73% ± 7% as compared to the stabilized samples (i.e. an overall mass yield of 0.64% ± 7% after stabilization and carbonization) was gained, while carbonization at 800°C resulted in a material yield of 43% ± 5% as compared to the stabilized samples (i.e. an overall mass yield of 0.38% ± 5%). No significant influence of the TiO<sub>2</sub> content, stabilization temperature, or maximum temperature is visible for all samples under examination.

These results underline the possibility to use the prepared TiO<sub>2</sub>/carbon nanofiber mats in the above-described applications, such as front electrodes in dye-sensitized solar cells,<sup>41</sup> for photocatalytic degradation,<sup>19–23</sup> and or as electrodes in different sorts of batteries.<sup>24–26</sup>

## Conclusion

TiO<sub>2</sub>/PAN nanofiber mats with different amounts of TiO<sub>2</sub> were prepared by electrospinning and afterwards stabilized at varying temperatures, approached with diverse heating rates, and finally carbonized at two different temperatures.

Despite the partly large amounts of TiO<sub>2</sub> in the nanofiber mats, the samples under investigation behave in most cases very similar to pure PAN nanofiber mats. This is also visible within this study by comparing the samples with and without TiO<sub>2</sub>.

An interesting effect occurs with respect to the sample morphology. While the TiO<sub>2</sub> seems to form bead-like agglomerations for larger amounts of TiO<sub>2</sub> after electrospinning, the TiO<sub>2</sub> becomes more and more visible also

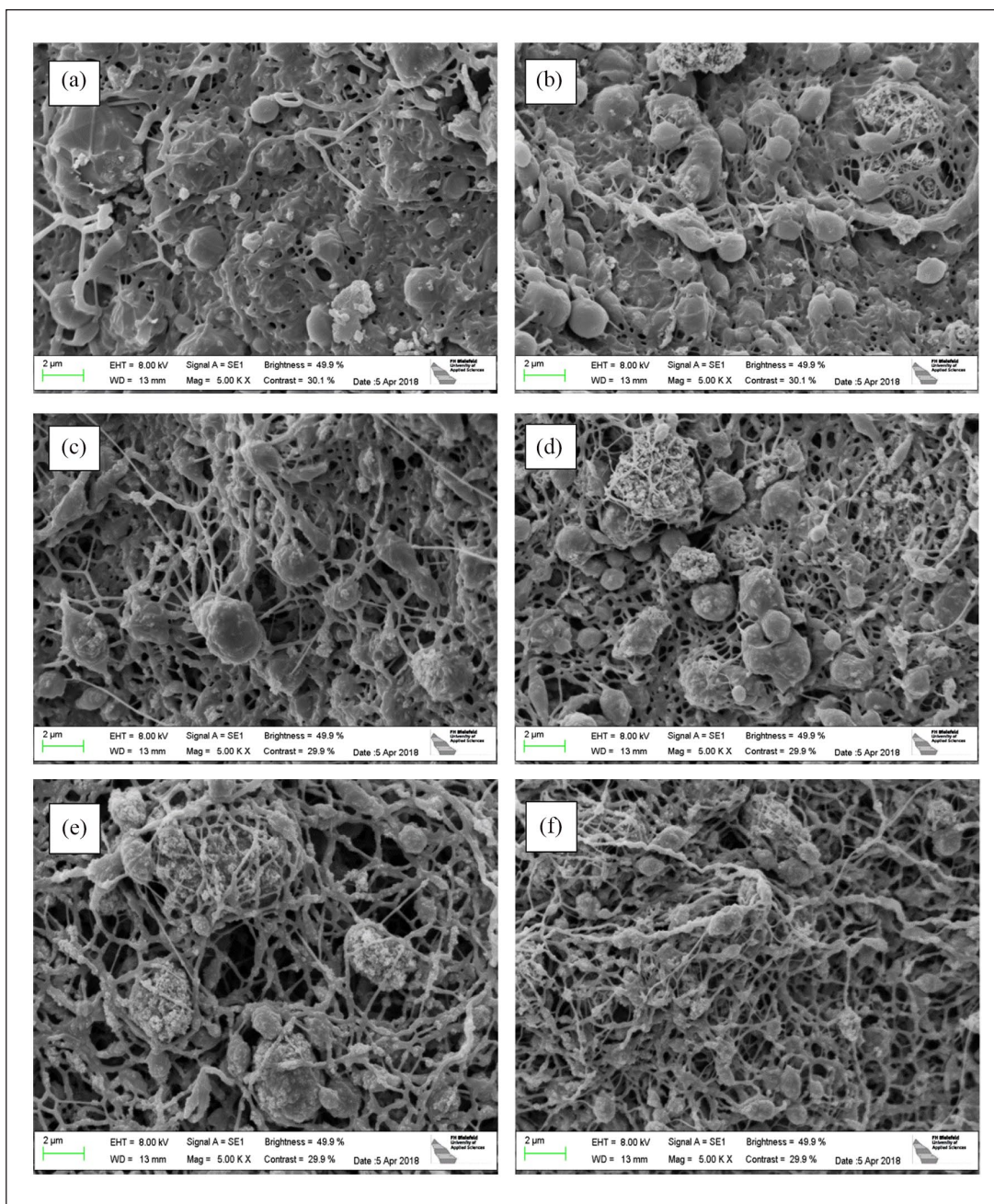


**Figure 4.** SEM images of PAN nanofiber mats with different amounts of TiO<sub>2</sub> after carbonization at different temperatures, approached with 10°C/min: (a) 2.2%/500°C, (b) 2.2% TiO<sub>2</sub>/800°C, (c) 6.2% TiO<sub>2</sub>/500°C, (d) 6.2% TiO<sub>2</sub>/800°C, (e) 10.2% TiO<sub>2</sub>/500°C, and (f) 10.2% TiO<sub>2</sub>/800°C.

along the fibers after stabilization and especially after carbonization. In addition, higher amounts of TiO<sub>2</sub> seem to stabilize the sample structure during stabilization. These findings are important for the applications of TiO<sub>2</sub>/carbon nanofibers in batteries or dye-sensitized solar cells, as they show that carbonization of TiO<sub>2</sub>/PAN nanofiber mats, needless electrospun from a DMSO solution, is possible and relatively high amounts of TiO<sub>2</sub> are even advantageous in maintaining the desired fibrous morphology, as opposed to pure PAN nanofiber mats.

Our study shows that electrospinning a blend of PAN and TiO<sub>2</sub> offers the possibility to create mats of nanofibers decorated with TiO<sub>2</sub> for possible use in dye-sensitized solar cells, for photodegradation of dyes, and similar applications.

#### Declaration of conflicting interests

The author(s) declared no potential conflicts of interest with respect to the research, authorship, and/or publication of this article.

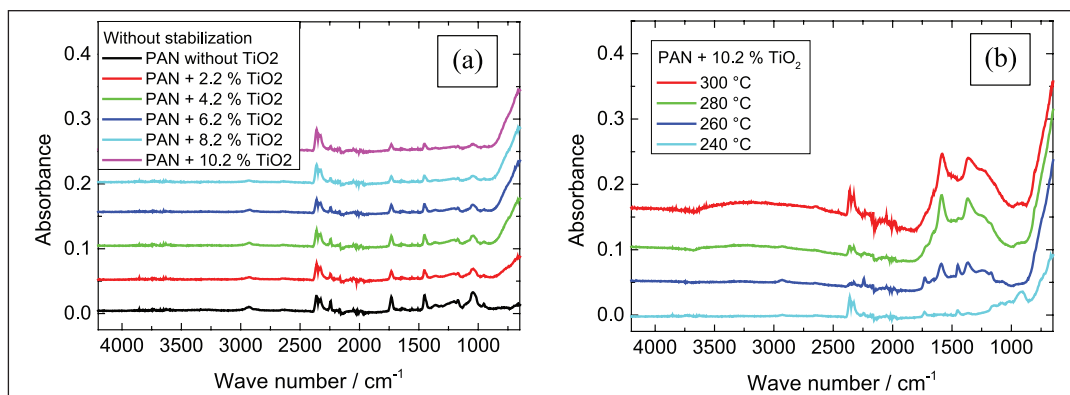


**Figure 5.** FTIR measurements: (a) PAN nanofiber mats with different amounts of  $\text{TiO}_2$  after electrospinning; (b) PAN nanofiber mats with the highest amount of  $\text{TiO}_2$  after stabilization at different temperatures.

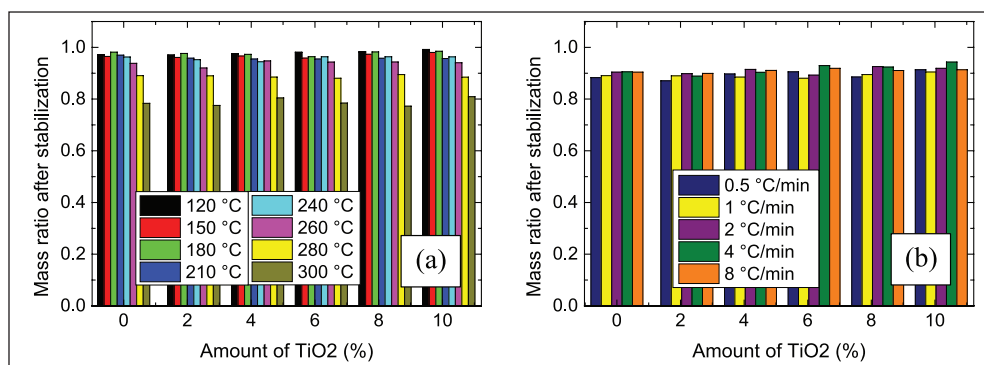


**Figure 6.** Ratio of masses after stabilization to masses before stabilization: (a) for different maximum temperatures, reached with a heating rate of  $1^\circ\text{C}/\text{min}$ ; (b) for different heating rates, approaching a maximum temperature of  $280^\circ\text{C}$ .

## Funding

The author(s) disclosed receipt of the following financial support for the research, authorship, and/or publication of this article: The study was partly funded by the HiF fund of Bielefeld University of Applied Sciences and the Junta de Andalucía for the group TEP-184. This article is funded by the Open Access Publication Fund of Bielefeld University of Applied Sciences and the Deutsche Forschungsgemeinschaft (DFG, German Research Foundation) – 414001623.

## References

- Subbiah T, Bhat GS, Tock RW, et al. Electrospinning of nanofibers. *J Appl Polym* 2005; 96: 557–569.
- Greiner A and Wendorff JH. Electrospinning: a fascinating method for the preparation of ultrathin fibers. *Angew Chem Int Edit* 2007; 46: 5670–5703.
- Li D and Xia Y. Electrospinning of nanofibers: reinventing the wheel? *Adv Mater* 2004; 16: 1151–1170.
- Lackowski M, Krupa A and Jaworek A. Nonwoven filtration mat production by electrospinning method. *J Phys Conf Ser* 2011; 301: 012013.
- Lemma SM, Esposito A, Mason M, et al. Removal of bacteria and yeast in water and beer by nylon nanofibrous membranes. *J Food Eng* 2015; 157: 1–6.
- Wang X, Kim YG, Drew C, et al. Electrostatic assembly of conjugated polymer thin layers on electrospun nanofibrous membranes for biosensors. *Nano Lett* 2004; 4: 331–334.
- Ruiz-Rosas R, Rosas JM, Loscertales IG, et al. Electrospinning of silica sub-microtubes mats with platinum nanoparticles for NO catalytic reduction. *Appl Catal B: Environ* 2014; 156–157: 15–24.
- García-Mateos FJ, Berenguer R, Valero-Romero MJ, et al. Phosphorus functionalization for the rapid preparation of highly nanoporous submicron-diameter carbon fibers by electrospinning of lignin solutions. *J Mater Chem A* 2018; 6: 1219–1233.
- Ashammakhi N, Ndreu A, Yang Y, et al. Nanofiber-based scaffolds for tissue engineering. *Eur J Plast Surg* 2012; 35: 135–149.
- Iatsunskyi I, Vasylenko A, Viter R, et al. Tailoring of the electronic properties of ZnO-polyacrylonitrile nanofibers: experiment and theory. *Appl Surf Sci* 2017; 411: 494–501.
- Che Othman FE, Yusof N, Hasbullah H, et al. Polyacrylonitrile/magnesium oxide-based activated carbon nanofibers with well-developed microporous structure and their adsorption performance for methane. *J Ind Eng Chem* 2017; 51: 281–287.
- García-Mateo FJ, Cordero-Lanzac T, Berenguer R, et al. Lignin-derived Pt supported carbon (submicron) fiber elec-

- trocatalysts for alcohol electro-oxidation. *Appl Catal B: Environ* 2017; 211: 18–30.
13. Guo J, Niu Q, Yuan Y, et al. Electrospun core-shell nanofibers derived Fe-S/N doped carbon material for oxygen reduction reaction. *Appl Surf Sci* 2017; 416: 118–123.
  14. Kim GH, Park SH, Birajdar MS, et al. Core/shell structured carbon nanofiber/platinum nanoparticle hybrid web as a counter electrode for dye-sensitized solar cell. *J Ind Eng Chem* 2017; 52: 211–217.
  15. Neisiany RE, Lee JKY, Khorasani SN, et al. Self-healing and interfacially toughened carbon fibre-epoxy composites based on electrospun core-shell nanofibres. *J Appl Polym Sci* 2017; 134: 44956.
  16. Sabantina L, Rodríguez-Cano MÁ, Klöcker M, et al. Fixing PAN nanofiber mats during stabilization for carbonization and creating novel metal/carbon composites. *Polymers* 2018; 10: 735.
  17. Grothe T, Wehlage D, Böhm T, et al. Needleless electrospinning of PAN nanofibre mats. *Tekstilec* 2017; 60: 290–295.
  18. Großerhode C, Wehlage D, Grothe T, et al. Investigation of microalgae growth on electrospun nanofiber mats. *AIMS Bioeng* 2017; 4: 376–385.
  19. Choi SK, Kim S, Lim SK, et al. Photocatalytic comparison of TiO<sub>2</sub> nanoparticles and electrospun TiO<sub>2</sub> nanofibers: effects of mesoporosity and interparticle charge transfer. *J Phys Chem C* 2010; 114: 16475–16480.
  20. Mishra S and Ahrenkiel SP. Synthesis and characterization of electrospun nanocomposite TiO<sub>2</sub> nanofibers with Ag nanoparticles for photocatalysis applications. *J Nanomater* 2012; 2012: 902491.
  21. Fu P, Luan Y and Dai X. Preparation of activated carbon fibers supported TiO<sub>2</sub> photocatalyst and evaluation of its photocatalytic reactivity. *J Mol Catal A: Chem* 2004; 221: 81–88.
  22. Song LX, Jing WR, Chen JJ, et al. High reusability and durability of carbon-doped TiO<sub>2</sub>/carbon nanofibrous film as visible-light-driven photocatalyst. *J Mater Sci* 2019; 54: 3795–3804.
  23. Seong DB, Son YR and Park SJ. A study of reduced graphene oxide/leaf-shaped TiO<sub>2</sub> nanofibers for enhanced photocatalytic performance via electrospinning. *J Solid State Chem* 2018; 266: 196–204.
  24. Yang Y, Liu QY, Cao M, et al. Enhanced electrochemical performance of  $\alpha$ -Fe<sub>2</sub>O<sub>3</sub> grains grafted onto TiO<sub>2</sub>-Carbon nanofibers via a vapor-solid reaction as anode materials for Li-ion batteries. *Appl Surf Sci* 2019; 463: 322–330.
  25. Nie S, Liu L, Liu JF, et al. Nitrogen-doped TiO<sub>2</sub>-C composite nanofibers with high-capacity and long-cycle life as anode materials for sodium-ion batteries. *Nano-micro Lett* 2018; 10: 71.
  26. He ZX, Li MM, Li YH, et al. Flexible electrospun carbon nanofiber embedded with TiO<sub>2</sub> as excellent negative electrode for vanadium redox flow battery. *Electrochim Acta* 2018; 281: 601–610.
  27. Shepa I, Mudra E, Vojtko M, et al. Preparation of highly crystalline titanium-based ceramic microfibers from polymer precursor blend by needle-less electrospinning. *Ceram Int* 2018; 44: 17925–17934.
  28. Deb H, Xiao SL, Morshed MN, et al. Immobilization of cationic titanium dioxide (TiO<sub>2</sub><sup>+</sup>) on electrospun nanofibrous mat: synthesis, characterization, and potential environmental application. *Fibers Polym* 2018; 19: 1715–1725.
  29. Yoo SH, Lee SI, Joh HI, et al. Highly effective photocatalysts based on carbon nanofibers decorated with TiO<sub>2</sub> and CdSe under visible light. *J Ind Eng Chem* 2018; 63: 27–32.
  30. Wang H, Huang XW, Li W, et al. TiO<sub>2</sub> nanoparticle decorated carbon nanofibers for removal of organic dyes. *Colloid Surface A* 2018; 549: 205–211.
  31. Su JF, Yang GH, Cheng CL, et al. Hierarchically structured TiO<sub>2</sub>/PAN nanofibrous membranes for high-efficiency air filtration and toluene degradation. *J Colloid Interf Sci* 2017; 507: 386–396.
  32. Chang GQ, Ullah W, Hu YF, et al. Functional carbon nanofibers with semi-embedded titanium oxide particles via electrospinning. *Macromol Rapid Comm* 2018; 39: 1800102.
  33. An H-R, An HL, Kim W-B, et al. Nitrogen-doped TiO<sub>2</sub> nanoparticle-carbon nanofiber composites as a counter electrode for Pt-free dye-sensitized solar cells. *ECS Solid State Lett* 2014; 3: M33–M36.
  34. Wang C, Yan EY, Huang ZH, et al. Fabrication of highly photoluminescent TiO<sub>2</sub>/PPV hybrid nanoparticle-polymer fibers by electrospinning. *Macromol Rapid Comm* 2007; 28: 205–209.
  35. Sabantina L, Klöcker M, Wortmann M, et al. Stabilization of PAN nanofiber mats obtained by needleless electrospinning using DMSO as solvent. *J Ind Text*. Epub ahead of print 15 January 2019. DOI: 10.1177/1528083718825315.
  36. Döpke C, Grothe T, Steblinski P, et al. Magnetic nanofiber mats for data storage and transfer. *Nanomaterials* 2019; 9: 92.
  37. Mólnar K, Szolnoki B, Toldy A, et al. Thermochemical stabilization and analysis of continuously electrospun nanofibers. *J Therm Anal Calorim* 2014; 117: 1123–1135.
  38. Cipriani E, Zanetti M, Bracco P, et al. Crosslinking and carbonization processes in PAN films and nanofibers. *Polym Degrad Stabil* 2016; 123: 178–188.
  39. Gergin I, Ismar E and Sarac AS. Oxidative stabilization of polyacrylonitrile nanofibers and carbon nanofibers containing graphene oxide (GO): a spectroscopic and electrochemical study. *Beilstein J Nanotech* 2017; 8: 1616–1628.
  40. Sabantina L, Wehlage D, Klöcker M, et al. Stabilization of electrospun PAN/gelatin nanofiber mats for carbonization. *J Nanomater* 2018; 2018: 6131085.
  41. Mamun A, Trabelsi M, Klöcker M, et al. Electrospun nanofiber mats with embedded non-sintered TiO<sub>2</sub> for dye-sensitized solar cells (DSSCs). *Fibers* 2019; 7: 60.